Decay path measurements for the 2.429 MeV state in ^{9}Be: Implications for the astrophysical $\alpha + \alpha + n$ reaction

P. Papka,* T. A. D. Brown,† B. R. Fulton, D. L. Watson, S. P. Fox, and D. Groombridge
Department of Physics, University of York, York YO10 5DD, United Kingdom

M. Freer, N. M. Clarke, N. I. Ashwood, N. Curtis, V. Ziman, P. McEwan, and S. Ahmed
School of Physics and Astronomy, University of Birmingham, Birmingham B15 2TT, United Kingdom

W. N. Catford, D. Mahboub, C. N. Timis, and T. D. Baldwin
School of Electronics and Physical Sciences, University of Surrey, Guildford GU2 7XH, United Kingdom

D. C. Weisser
Department of Nuclear Physics, Australian National University, Canberra ACT 0200, Australia
(Received 9 October 2006; revised manuscript received 15 January 2007; published 12 April 2007)

An experiment was performed at the Australian National University to study the ^{9}Be(^{6}Li,^{6}Li)^{9}Be$^* \rightarrow \alpha + \alpha + n$ reaction. This experiment was designed to study the breakup of ^{9}Be, in an attempt to quantify the contribution played by the ^{5}He + α and ^{8}Be$^{2^+}$ + n channels for the low lying excited states. This information is required in order to resolve uncertainties in the $\alpha + \alpha + n \rightarrow {}^9$Be reaction rate in high-energy and neutron-rich astrophysical environments such as supernovae. Angular correlation measurements have been used to deduce that the 2.429 MeV state breaks up almost exclusively via the ^{8}Be$^{2^+}$ channel. This method of identifying the break-up channel resolves the problem of distinguishing between the ^{8}Be$^{2^+}$ and ^{5}He$^{g.s.}$ channels which are kinetically identical at this excitation energy.

DOI: 10.1103/PhysRevC.75.045803 PACS number(s): 26.30.+k, 21.10.−k, 25.60.Gc, 27.20.+n

I. INTRODUCTION

The structure of the ^{9}Be nucleus has long been a matter of interest, in particular the strength of any three-body $\alpha + \alpha + n$ cluster configuration. This possibility has received renewed attention recently, since it is believed that in neutron-rich astrophysical environments, such as a core-collapse supernovae, the three-body reaction $\alpha + \alpha + n \rightarrow {}^9$Be followed by ^{9}Be($\alpha$,$n$)^{12}C may provide a route for building up the heavy elements and triggering the r-process [1–4]. The first stage can proceed by two routes, either $\alpha + \alpha \rightarrow {}^8$Be followed by ^{8}Be + $n \rightarrow {}^9$Be, or $\alpha + n \rightarrow {}^5$He followed by ^{5}He + $\alpha \rightarrow {}^9$Be. In the absence of any experimental evidence for the ^{5}He + α configuration, calculations are invariably done assuming only the ^{8}Be + n route, the argument being that the different lifetimes of the ^{8}Be and ^{5}He intermediate states (10^{-16}s and 10^{-21}s, respectively) should favor the former. However, calculating the rate properly requires a knowledge of the relative strength of the ^{8}Be + n and ^{5}He + α cluster configurations in ^{9}Be. The key states in this context are those just above the particle threshold, in particular those at E_x = 1.684 MeV ($1/2^+$) and 2.429 MeV ($5/2^-$), see Fig. 1.

Previous calculations of the three-body rate [6–9] assumed that the reaction proceeded only via the ^{8}Be$^{0^+}$ + n channel and through the various low-lying states in ^{9}Be. Several recent theoretical studies have explored the cluster configuration for these states using microscopic cluster model calculations [10, 11]. The cluster models include two two-body configurations, ^{8}Be + n and ^{5}He + α, and also allow the possibility of the ^{8}Be being in the broad $J^\pi = 2^+$ state at $E_x = 3.04$ MeV. A common feature of the model calculations is that the ^{5}He + α configuration is important even for the low-lying states and indeed becomes dominant at higher excitation energies.

Following a recent measurement of ^{9}C β-decay [12], which showed that the analogues to some of the ^{9}Be states had large ^{5}Li widths, Buchmann *et al.* [13] recalculated the rate including the ^{5}He + α and ^{8}Be$^{2^+}$ + n channels. While the latter was suggested not to play an important role, the former had a considerable effect on the reaction rate at higher temperatures. In a separate reevaluation by Sumiyoshi *et al.* [14], to incorporate revised neutron widths, these authors also drew attention to the need to consider the ^{5}He + α channel. However, as the authors of both calculations point out, this is hampered by a severe lack of experimental information on the partial widths for the various channels.

In a recent investigation [15], Grigorenko and Zhukov include the ^{5}He + α channel and find that it only makes a small contribution. Note that 93–95% of the strength proceeds "democratically" and the ^{8}Be$^{2^+}$ + n is not considered in this work. The democratic decay has been investigated by several authors [16,17] as an alternative route to the sequential decay.

Experimental information on the cluster configurations in ^{9}Be have come from break-up measurements, i.e., studies of the decay of the states in ^{9}Be to the $\alpha + \alpha + n$ channel. The

*Present address: iThemba LABS, PO Box 722, Somerset West 7129, South Africa.
†Present address: CENPA, Box 354290, University of Washington, Seattle, WA 98115, USA.

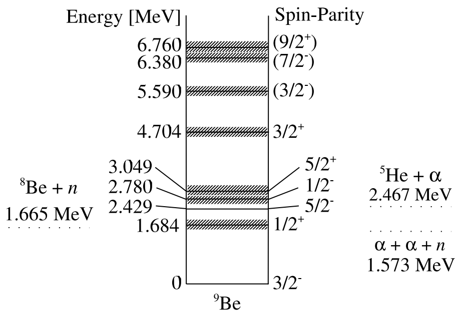

FIG. 1. The low-lying excited states in ^{9}Be derived from proton scattering measurements made by Dixit *et al.* [5]. The states at $E_x = 2.429$ and 6.380 MeV are part of the ground state rotational band.

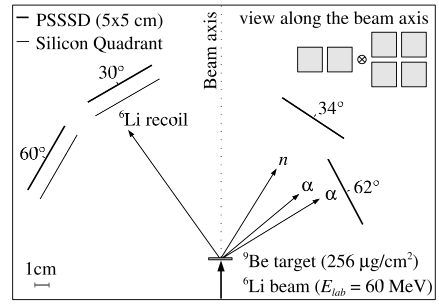

FIG. 2. The experimental setup.

excited ^{9}Be states have been prepared in various ways, recent examples include through β-decay [18], in scattering reactions [19] or by photodisintegration [20]. Most measurements confirm that the 2.429 MeV state has a branching ratio to the $^8\mathrm{Be}^{0^+} + n$ channel of about 7% [21,22], but cannot determine whether the remaining strength is in the $^8\mathrm{Be}^{2^+} + n$ or $^5\mathrm{He} + \alpha$ channels. It is however reported in [23], with no justification, that a ratio of 2:1 can be accounted for the two channels, respectively. The main problem is that because the decays are below threshold, the energy shared between the three particles is small and with this restricted phase space the kinematics for decay through the two configurations are identical, i.e., the energy correlations between the decay particles are the same irrespective of the intermediate step in the decay [24]. This is certainly the case in inclusive measurements (i.e., where only α-particle singles or neutron singles are measured) but is also the case in exclusive measurements where coincident detection of the decay particles is achieved. This was nicely illustrated in calculations shown in [25].

In this paper we have carried out an exclusive measurement of the breakup of ^{9}Be excited through inelastic scattering and show that by exploring another aspect of the correlation between the decay particles, the angular correlation, this restriction can be removed. This approach has recently been used to investigate β-delayed breakup from ^{9}Be [18], although this measurement did not include the 2.429 MeV state (because of the β-decay selection rules only low spin, negative parity states can be populated). This has enabled us, for the first time, to show that the remaining strength in the decay of the 2.429 MeV state is to the $^8\mathrm{Be}^{2^+} + n$ channel and that the partial width of the $^5\mathrm{He} + \alpha$ channel is very small.

II. EXPERIMENTAL METHOD AND ANALYSIS

The experiment was performed using the 14UD pelletron tandem accelerator at the Australian National University during April 2003. The experiment was designed to study the inelastic scattering of ^{6}Li nuclei from a ^{9}Be target and the subsequent breakup of the excited ^{9}Be nuclei. The detection technique for this experiment required that the ^{6}Li recoils were detected and identified. By also detecting and identifying the two corresponding break-up α particles for each break-up event, it is then possible to reconstruct the missing momentum of the undetected neutron. The reaction kinematics should then be fully defined, allowing the complete reconstruction of the break-up event and identification of the state in ^{9}Be that was populated. A ^{6}Li beam at $E_{\mathrm{lab}} = 60$ MeV was focused onto a ^{9}Be target (256 μg/cm^2). Data were taken for approximately 92 hrs with a beam current of between $\mathrm{I}_{\mathrm{beam}} \approx$ 2–5 enA. For the purposes of detecting the particles arising from the breakup of ^{9}Be, four position sensitive silicon-strip detectors (PSSSDs) were used. Two detector telescopes, both consisting of the combination of a silicon quadrant detector (≈ 65 μm thick) mounted in front of a PSSSD (≈ 500 μm thick), were used to detect and identify the recoil lithium particles. Figure 2 illustrates the setup inside the experimental chamber. The position of the detectors relative to the target are indicated therein and were chosen based on efficiency results obtained from Monte Carlo simulations.

Events comprising a ^{6}Li in one of the telescopes, identified from the characteristic locus in a $E\Delta E$ plot, coincident with two hits in the strip detectors were selected for analysis. Events where two adjacent strips fired were rejected, since such signals can be produced by a single particle entering an interstrip gap on the detector and inducing a signal on the adjacent strips. Assuming that the two strip detector hits were α particles, the missing momentum and energy of the neutron could be calculated and hence the Total final state Kinetic Energy (TKE) determined ($E_{\mathrm{TKE}} = E_{\alpha_1} + E_{\alpha_2} + E_n + E_{^6Li}$). A clear peak is observed in the TKE spectrum at an energy of $E_{\mathrm{TKE}} = 58.3$ MeV, which is consistent with the beam energy of $E_{\mathrm{lab}} = 60$ MeV, minus the Q-value for breakup ($Q = -1.57$ MeV) and the energy loss in the target ($E_L \approx 100$ keV). Gating on this peak ensures that we select on genuine $\alpha + \alpha + n$ break-up events.

Having now selected the required events, we can calculate the relative energy $E_{\alpha\alpha}$ between the α particles. This is shown in Fig. 3 and reveals three distinct features. The narrow peak at $E_{\alpha\alpha} = 92$ keV (Q-value of ^{8}Be breakup) corresponds to breakup via the $^8\mathrm{Be}^{0^+}$. The broad peak at around $E_{\alpha\alpha} \approx 3$ MeV corresponds to the decay of excited states in ^{9}Be with an excitation energy $E_x > 5$ MeV. It has been shown in previous work that the $^5\mathrm{He} + \alpha$ channel contributes significantly at higher excitation energy [26,27]. The broad distribution can reflect two contributions; breakup via the $J^\pi = 2^+$ first excited state in ^{8}Be and breakup via the $J^\pi = 3/2^-$ ground state in ^{5}He.

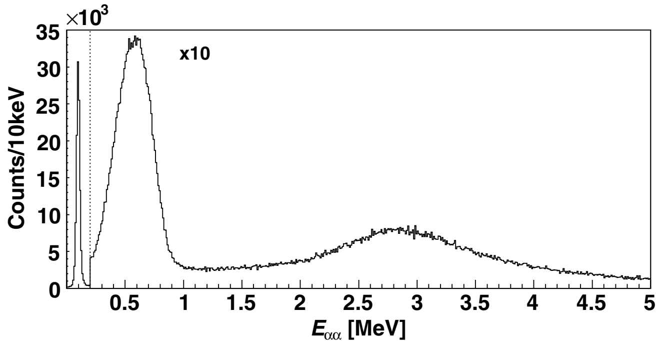

FIG. 3. α-α relative energy spectrum for events with 57 MeV < E_{TKE} < 60 MeV.

The third feature in the spectrum, the bump lying at about $E_{\alpha\alpha} \approx 600$ keV, is of most interest since it has been strongly identified with the 2.429 MeV state in the literature [19,24,25]. This "bump" does not correspond to an energy state in ^{8}Be, but it has been suggested [23] that these events reflect breakup via the tail of the broad first excited state in ^{8}Be ($\Gamma = 1.5$ MeV) or the tail of the ground state in ^{5}He ($\Gamma = 648$ keV). The shape would reflect a complex interplay between the decreasing strength in the low energy tail of the state (favoring higher energies) and the phase space (favoring lower energies). Gating on these features in the $E_{\alpha\alpha}$ spectrum enables us to identify which states in ^{9}Be decay to particular channels. Figure 4(a) illustrates the ^{9}Be excitation energy spectrum reconstructed for $^8\mathrm{Be}^{0^+}$ events and Fig. 4(b) that for the "bump" at $E_{\alpha\alpha} \approx 600$ keV. The former shows excitation of the known states in ^{9}Be indicated by the three-Gaussian fit on the spectrum showing the contributions of the states at $E_x = 1.68$, 2.429, and 3.05 MeV.

Due to the width of the states and the intrinsic resolution, the fit of Fig. 4(a) is not trivial. The width and position of the 2.429 MeV peak is deduced from the fit of Fig. 4(b) and the only free parameter for this Gaussian in Fig. 4(a) is the weight. The contribution at low excitation energy should come from the 1.68 MeV state but the best fit is obtained with a centroid located at $E_x = 2.0$ MeV. The contributions from the 2.78 and 3.05 MeV states cannot reasonably be deconvoluted, consequently, they are merged in one component found to be located at $E_x = 3.1$ MeV. The background results from a fit for excitation energy between $E_x = 4$–8 MeV extrapolated to lower excitation energy. This background includes the broad states at $E_x = 4.7$ and around 6.38 MeV, and a flat component vanishing to zero at $E_x = 1.6$ MeV.

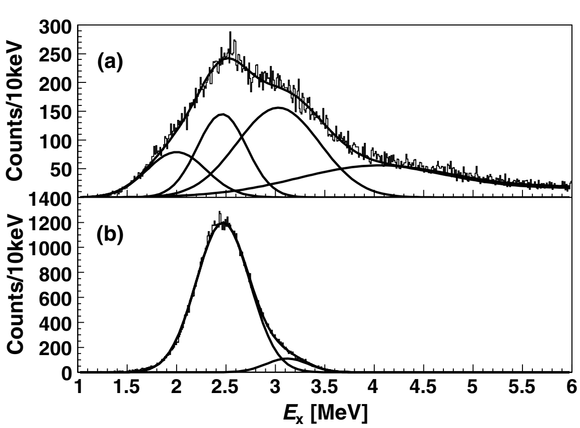

FIG. 4. ^{9}Be excitation energy spectra derived from ^{6}Li recoils for (a) $^8\mathrm{Be}^{0^+}$ events and (b) with 0.2 MeV < $E_{\alpha\alpha}$ < 1.0 MeV and 58 MeV < E_{TKE} < 59 MeV.

When the selection is made on the 600 keV bump, the spectrum in Fig. 4(b) is seen, illustrating a dominant contribution from the state at $E_x = 2.429$ MeV. Events which breakup via the 2.78/3.05 MeV states have been identified in the high energy tail of the Gaussian. They were deconvoluted with a two-Gaussian fit and are estimated to account for approximately 7±1% of the events in the 600 keV bump. Note that events corresponding to the neutron transfer reaction $^9\mathrm{Be}(^6\mathrm{Li},^7\mathrm{Li}^*)^8\mathrm{Be}^* \rightarrow {}^6\mathrm{Li} + n + 2\alpha$, which has an identical Q-value, could fall within the TKE window. The excitation energy in ^{7}Li has been reconstructed and only the first excited state above the neutron threshold has been identified at $E_x = 7.459$ MeV. This contamination appears in the spectrum only at high excitation energy and can be removed with appropriate selections.

III. INTERPRETATION OF THE RESULTS

A. The simulation code

For the purposes of identifying the kinematic signatures of the different decay channels, a Monte Carlo code SIMSORT [28] has been written which simulates the inelastic scattering of the ^{6}Li beam from the ^{9}Be target, the subsequent breakup of the ^{9}Be nuclei and the detector response to the exit channel particles. The user can define the exact nature of the break-up path for the purposes of a simulation: the excited state populated in ^{9}Be and whether breakup occurs via $^8\mathrm{Be}^{0^+}$, $^8\mathrm{Be}^{2^+}$, or $^5\mathrm{He}^{g.s.}$. SIMSORT assumes an isotropic center-of-mass (c.m.) distribution for each of the break-up stages, although an anisotropy can be introduced (see next section). However, the scattering distribution for the ^{6}Li recoils used in the code was derived from the experimental results and reconstructed from the two telescopes. The code also contains details of the detector setup, threshold detection energies, the expected energy resolution for the silicon detectors (FWHM ≈ 200 keV), the position resolution of the PSSSDs (FWHM ≈ 0.5 mm across a strip), etc. For the sake of consistency with the analysis of the real data, SIMSORT uses an identical data sort process, i.e., events detected in adjacent PSSSD strips are rejected, identical gates are applied, α particles are randomly labeled 1 and 2, etc.

Figure 5 illustrates a velocity vector diagram of the break-up particles and intermediate ^{8}Be and ^{5}He resonances in the ^{9}Be c.m. frame. The solid lines represent the decay paths via the $^8\mathrm{Be}^{2^+} + n$ channel and the dotted and dashed lines via the two solutions of the $^5\mathrm{He} + \alpha$ channel. The relative energies between particles can be calculated as follows: $E_{\mathrm{rel}} = M_\mu V_{\mathrm{rel}}^2/2$ where V_{rel} is the velocity vector measured between the particles and M_μ is the reduced mass. The energy available for each decay depends upon the excitation energy E_x of the parent state and the Q-value of the resulting decay channel. The relative energy between two daughter particles

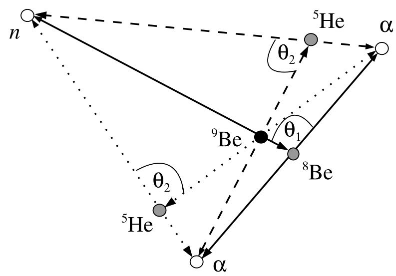

FIG. 5. Illustration of the angles θ_1 and θ_2 used to establish angular correlations for breakup via the ^{5}He$^{g.s.}$ and the ^{8}Be$^{2^+}$ resonances. The diagram is drawn in the ^{9}Be c.m. frame and represents the ^{8}Be$^{2^+}$ + n (solid) and ^{5}He$^{g.s.}$ + α (dotted and dashed) channels. The grey circles represent the intermediate resonances and the white circles the final break-up particles. The relative energies summed in each of the three decays are consistent with the available energy $E_a = E_x + Q = 0.858$ MeV.

in their c.m. frame can also be written $E_{\rm rel} = E_x + Q$. The Q-values for the first stage of sequential ^{9}Be breakup are $Q = -1.665$ and -2.467 MeV for decay via ^{8}Be and ^{5}He, respectively. For breakup to the ^{8}Be$^{2^+}$ state this Q-value is effectively 3 MeV lower. Given an excitation energy of $E_x = 2.429$ MeV, breakup to the ^{5}He$^{g.s.}$ (Γ = 648 keV) and the ^{8}Be$^{2^+}$ ($\Gamma = 1.5$ MeV) states is only possible due to the broad width of these intermediate states. The relative energy between the particles in the first step emission thus depends on the penetrability of the particle through the Coulomb and/or centrifugal barrier and the phase space defined by the state in the residual nucleus, we return to this point later.

The vector diagram, see Fig. 5, shows a specific decay for an available energy equally shared between the two stages of the breakup. The kinematics is identical for the two channels and the relative energy at each stage of the decay can span from $E_{\rm rel} = 0$ to E_a, with the condition that the sum of the relative energies is equal to E_a the available energy. As a consequence, there is no obvious signature for either the ^{5}He$^{g.s.}$ or the ^{8}Be$^{2^+}$ decay channel which could be expected in the α-^{5}He ($E_{\alpha ^5{\rm He}}$) or n-^{8}Be ($E_{n ^8{\rm Be}}$) relative energy spectra. However, the existence of angular correlations may provide a solution for distinguishing the two different break-up paths.

B. Angular correlations

The following multistep angular correlation formalism is described in detail by Biedenharn and Rose [29], and has been used successfully to assign spins for ^{9}Be and ^{9}B states studied using β-delayed breakup [30]. The following analysis is based on the same approach. The emission of particles in cascade from the same nucleus yields a correlation between their relative propagation directions. A correlation function $W(\theta)$,

$$W(\theta) = \sum_{\nu} A_\nu P_\nu(\cos\theta), \tag{1}$$

can be defined for two such particles emitted in cascade [29]. This function represents the probability that emission will occur at an angle between the first emitted particle and the direction of a secondary emission. Figure 5 illustrates the definition of the angles for the case of breakup via ^{8}Be (θ_1) and for the case of breakup via ^{5}He (θ_2). The function $W(\theta)$ is a sum of Legendre Polynomials $P_\nu(\cos\theta)$. The coefficient associated with each Legendre polynomial A_ν and the length of the sum ν can be calculated from the angular momenta of the initial, intermediate and final particles [30]:

TABLE I. Values of spins and angular momenta for ^{5}He$^{g.s.}$ + α and ^{8}Be$^{2^+}$ + n sequential decays.

	j_1	j	j_2	l_1	l_2	$\nu_{\rm max}$
^{5}He$^{g.s.}$ + α	5/2	3/2	±1/2	2	1	2
^{8}Be$^{2^+}$ + n	5/2 ± 1/2	2	0	1	2	2

$$A_\nu = F_\nu(l_1 j_1 j) b_\nu(l_1 l_1) F_\nu(l_2 j_2 j) b_\nu(l_2 l_2), \tag{2}$$

$$b_\nu(ll) = \frac{2l(l+1)}{2l(l+1) - \nu(\nu+1)}, \tag{3}$$

$$\begin{aligned} &0 \leqslant \nu_{\rm max} \leqslant 2j; \quad 0 \leqslant \nu_{\rm max} \leqslant 2(l_1)_{\rm max}; \\ &0 \leqslant \nu_{\rm max} \leqslant 2(l_2)_{\rm max}. \end{aligned} \tag{4}$$

The parameters j_1, j, and j_2 are the spins of the initial, intermediate, and final states, respectively, and $l_{1,2}$ are the orbital angular momenta associated with the initial and final states. These values determine the length $\nu_{\rm max}$ of the sum following Eq. (4). F_ν is a geometrical function, determined by the angular momenta in which the numerical values are given in Biedenharn and Rose [29]. The values taken for all those parameters are given in Table I. $l_{1,2}$ have a unique solution for the ^{5}He + α channel but for the decay via ^{8}Be$^{2^+}$ the orbital angular momentum at the first step decay can be $l_1 = 1$ or 3. The decay from the highest angular momenta is hampered due to the centrifugal barrier [29] and can be neglected. This is illustrated in Fig. 6 with the calculation of the penetrability folded with the Lorentzian shape of the ^{8}Be$^{2^+}$ state for the

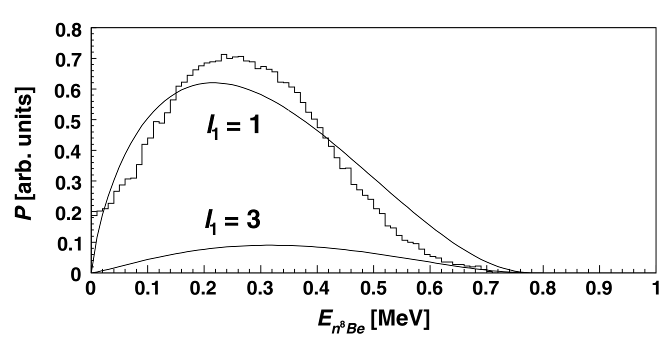

FIG. 6. Calculated $E_{n^8{\rm Be}}$ profiles (solid curves) for $l_1 = 1$ and $l_1 = 3$. The histogram is the profile extracted from the simulation obtained as the best reproduction of the real set of data. The histogram is normalized to the calculated distribution for comparison.

two values of l_1 (solid lines). The parameters for the $^8\mathrm{Be}^{2^+}$ + n channel are calculated with $j_1 = 5/2 \pm 1/2$ due to the neutron emission. Most of the application require the extreme values for the correlation but the two possible combinations of spin and angular momentum interfere and the $A_{0,2}$ parameters should be calculated accordingly. The $b_\nu(ll)$ coefficients are calculated following Eq. (3). For the case of the state at $E_x = 2.429$ MeV ($5/2^-$) the correlation function reduces to the following form for breakup via $^5\mathrm{He}^{\mathrm{g.s.}}$ and $^8\mathrm{Be}^{2^+}$ channels:

$$W(\theta) = A_0 + \tfrac{1}{2}A_2(3\cos^2\theta - 1). \tag{5}$$

This 3D probability distribution for θ can be projected in 1D by multiplying Eq. (5) by $\sin\theta$. By incorporating the 3D probability distribution for θ into SIMSORT, thereby introducing an anisotropy into the c.m. break-up distribution, the $W(\theta)$ profile can be compared with the distribution reconstructed from experimental data.

C. $^8\mathrm{Be}^{0^+}$ + n breakup

The measurement of the breakup via $^8\mathrm{Be}^{0^+}$ is straightforward due to the narrow peak at $E_{\alpha\alpha} = 92$ keV corresponding to the ground state of the unbound ^{8}Be. The deconvolution of the three states in Fig. 4(a) reveals that $11 \pm 2\%$ of the 2.429 MeV state decays via $^8\mathrm{Be}^{0^+}$. This measurement is consistent with previous results reported in [21,22], though it is slightly higher. However, a different method applied on the same data [27] gives a ratio of $6 \pm 1\%$ which is in perfect agreement with [21,22]. The former result should not be considered accurate due to a nontrivial deconvolution of the broad states in the low excitation energy region of Fig. 4(a).

D. $^8\mathrm{Be}^{2^+}$ + n breakup

As alluded to earlier, the $E_{n^8\mathrm{Be}}$ profile to be used for the simulation is very important. The penetrability, $P(E)$, has been calculated including simply the centrifugal barrier when emitting a neutron with an energy $E_{n^8\mathrm{Be}} = 0$ to 0.76 MeV. This distribution is folded with the Lorentzian shape of the $^8\mathrm{Be}^{2^+}$ state and the penetrability of the two α particles through the Coulomb and centrifugal barriers in the $^8\mathrm{Be}^{2^+}$ decay. The result of this calculation is shown in Fig. 6 (solid lines) for the two possible values of l_1. However, such a calculation might not be relied upon as more sophisticated considerations would be required including the possible interference with the overlapping states. Therefore, we used the experimental data to deduce the best $E_{n^8\mathrm{Be}}$ profile by adjusting the shape used in the simulation to reproduce the measurements.

$E_{\alpha\alpha}$ does not depend on the θ_1 angular distribution at the first step emission in the ^{8}Be + n exit channel. As a consequence, the direction taken by the neutron has no influence on the $E_{\alpha\alpha}$ relative energy as the ^{8}Be decays at the second step of the decay. The $E_{\alpha\alpha}$ spectrum is reconstructed in the ^{8}Be c.m. frame and is only altered by the experimental set-up response. Therefore, it is possible to extract from the simulation the energy distribution required for the first step

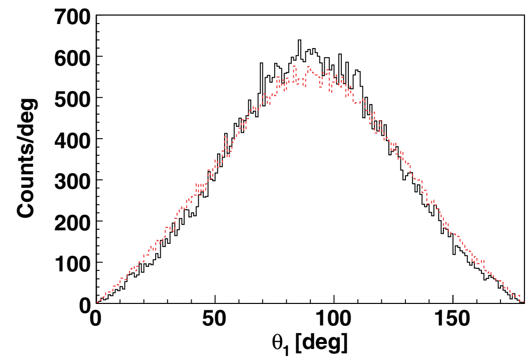

FIG. 7. (Color online) θ_1 spectrum reconstructed for real break-up data (solid) and simulated data (dotted) with $E_{\alpha\alpha} > 0.2$ MeV and the ^{9}Be excitation energy 2.2 MeV $< E_x <$ 2.6 MeV. Data are simulated with the θ_1 profile described by $W(\theta_1)\sin(\theta_1)$ where $A_0 = 0.848$ and $A_2 = -0.302$, assuming breakup via $^8\mathrm{Be}^{2^+}$ and population of the 2.429 MeV state.

emission. This profile is then used to perform the complete simulation of the reaction and all parameters deduced from experimental data are reproduced in the simulation.

The histogram of Fig. 6 is the result of the adjustment which is fairly close to the calculation (solid curve) for $l_1 = 1$. The barrier is seen around $E_b \approx 250$ keV and the maximum energy is close to the available energy $E_a = E_x + Q = 0.76$ MeV. Now that we have the correct profile for the relative energy in the simulation, we can compare the predicted angular correlations to the measured ones. Figure 7 illustrates a 1D distribution plot reconstructed from experimental data (solid). A larger energy gate on the ^{9}Be excitation energy of $\Delta E_x = 400$ keV has been used on this occasion to boost the statistics.

The $A_{0,2}$ parameters of Eq. (5) have been calculated using Eq. (2) assuming breakup via the $^8\mathrm{Be}^{2^+}$ state and including the initial spin of the 2.429 MeV state $J^\pi = 5/2^-(\pm 1/2)$. We assumed that the spin distribution of j_1 is equally shared between the two values $j_1 = 2$ and 3. The predicted distribution, $W(\theta)$, defined by the resulting parameters $A_0 = 0.848$ and $A_2 = -0.302$, is plotted in Fig. 7 (dotted) and is a very good reproduction of the experimental distribution. A fit was also performed to quantify the spin distribution. The result suggests that $65 \pm 1\%$ of the events decay via spin $j_1 = 2$. The Legendre polynomial parameters, in this case, are found to be $A_0 = 0.783$ and $A_2 = -0.433$. This ratio should not be considered accurate as we omitted to include the $l_1 = 3$ orbital angular momentum in the fit. It shows, however, that the assumption of an equally shared spin distribution is acceptable.

This result suggests that the vast majority of the break-up events that populate the 2.429 MeV state, with $E_{\alpha\alpha} > 200$ keV, breakup via the $^8\mathrm{Be}^{2^+}$ state.

E. ^{5}He + α breakup

The fact that the experimental energy and angular distributions can be understood using the $^8\mathrm{Be}^{2^+}$ + n channel alone is not in itself sufficient evidence that the ^{5}He + α channel does not contribute. However, in this section, we show that any such contribution must be small, otherwise discrepancies with the measured angular correlations would arise. Unfortunately, two complications arise when analyzing this channel: uncertainty over which α particle is correlated with the neutron, which in turn leads to a lack of knowledge of the first stage break-up relative energy and angular distributions. These points are discussed below.

As mentioned earlier, the choice of the α particle used to reconstruct an event is random. As a consequence approximately 50% of the experimental data will be incorrectly reconstructed assuming the identity of the break-up path is unknown. However, this choice is crucial for the correct reconstruction of the $E_{\alpha^5\mathrm{He}}$ and θ_2 distributions. In a simulation, the incorrect α particle will be chosen to reconstruct the ^{5}He nucleus for approximately half of the simulated events. The resulting distributions, produced by SIMSORT, will therefore consist of an approximately 50/50 mix of events that have been correctly and incorrectly reconstructed as expected for real events.

To ensure a fair comparison between the simulated and experimental data, the $E_{\alpha^5\mathrm{He}}$ distribution for simulated events must be a good reproduction of the real distribution reconstructed assuming breakup via ^{5}He. Therefore, an accurate description of the $E_{\alpha\alpha}$ energy profile should yield an accurate description of $E_{\alpha^5\mathrm{He}}$. However, in the case of the $^5\mathrm{He}^{\mathrm{g.s.}}$ events, the $E_{\alpha\alpha}$ profile depends also upon the break-up angular distribution of the neutron, which is responsible for giving a recoil kick to the α particle emitted in the second stage of the breakup.

In the previous section, we are able to analyze the $^8\mathrm{Be}^{2^+} + n$ channel by using the experimental data to constrain the relative energy, but this is not possible for the $^5\mathrm{He} + \alpha$ channel. Therefore the analysis has to be carried out with assumptions on θ_2. Using Eq. (5), the parameters of the $W(\theta)$ function are predicted to be $A_0 = 0.737$ and $A_2 = -0.526$. Using those parameters, the $E_{\alpha^5\mathrm{He}}$ profile can be extracted from the simulation using the same method. The resulting distribution is shown in Fig. 8 (histogram) which reproduces with a good agreement the 1D projections reconstructed in both channels.

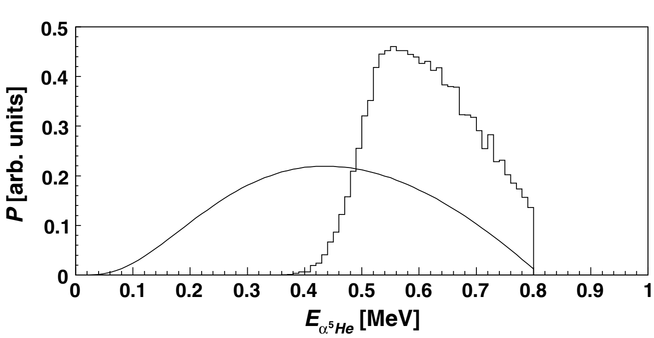

FIG. 8. $E_{\alpha^5\mathrm{He}}$ profile deduced from calculation (solid curve) and from simulation (histogram) assuming a $W(\theta)$ function defined by the parameters $A_0 = 0.737$ and $A_2 = -0.526$. The distribution obtained from simulation is normalized to the calculation for comparison.

The penetrability function is calculated as previously described for the $^8\mathrm{Be}^{2^+} + n$ decay. The Coulomb barrier is now included, the centrifugal barrier is calculated for $l_1 = 2$ and the resulting penetrability is folded with the phase space in the residual $^5\mathrm{He}^{\mathrm{g.s.}}$. There is a striking difference between the calculation, shown in Fig. 8 (solid curve), and the $E_{\alpha^5\mathrm{He}}$ profile obtained from the simulation (histogram). The position of the 600 keV bump can be understood by means of the $^5\mathrm{He} + \alpha$ channel only if the $E_{\alpha^5\mathrm{He}}$ distribution lies at higher energy than predicted by the calculation. This is consistent with previous work [25] where the 600 keV bump is shifted to lower energy when simulating the $^5\mathrm{He} + \alpha$ channel using the formalism of [22].

The comparison between the calculation and the relative energy tends to show that the $^5\mathrm{He} + \alpha$ channel is unlikely. However, such a conclusion should be drawn carefully. As already mentioned in the previous section, possible interference with neighboring broad states should be included in the calculations which could lead to different result. In order to investigate the possible contribution of the $^5\mathrm{He} + \alpha$ channel, we have carried out an analysis of the energy dependence of θ_1.

The 2D spectra $E_{\alpha\alpha}$ versus θ_1 in Figs. 9(a) and 9(b) show a striking inconsistency when the $^5\mathrm{He} + \alpha$ channel is simulated. The discrepancy is shown in Figs. 9(c) and 9(d) where 1D projections of θ_1 are plotted with selections on $E_{\alpha\alpha}$. Each spectrum has been obtained with gates on the α-α relative energy from $E_{\alpha\alpha} = 0.2$ to 0.8 MeV with a step $\delta E_{\alpha\alpha} = 100$ keV and normalized in order to show the energy dependence of the angular distribution. $E_{\alpha\alpha} > 0.8$ MeV, which corresponds to the lowest values of $E_{n^8\mathrm{Be}}$, is not included due to the

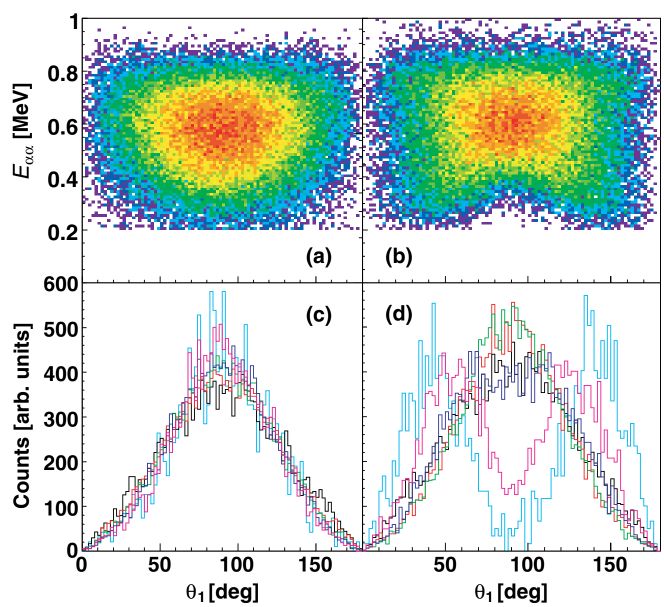

FIG. 9. (Color online) 2D projections of $E_{\alpha\alpha}$ versus θ_1 (a),(b) and 1D projections of θ_1 plotted with selections on $E_{\alpha\alpha} = 0.2$ to 0.8 MeV with a step of $\delta E_{\alpha\alpha} = 100$ keV (c),(d). The spectra (a) and (c) result from experimental data and (b),(d) from simulated data considering the $^5\mathrm{He} + \alpha$ exit channel with parameters $A_0 = 0.737$ and $A_2 = -0.526$.

TABLE II. Theoretical and experimental partial decay widths for the three sequential decay channels considered in this work.

	Reference	$^8\mathrm{Be}^{0^+} + n$	$^8\mathrm{Be}^{2^+} + n$	$^5\mathrm{He}^{\mathrm{g.s.}} + \alpha$
Theory	[10]	0.8%	92.7%	6.5%
Experiment	(this work)	11±2%	$86.5^{+4.5}_{-2.0}$%	<2.5%
Systematics	[21,22,27]	≈7%	-	-

larger uncertainty on the neutron position and subsequently θ_1. Figure 9(c) shows that θ_1 measured in the experimental data has no energy dependence and each spectrum has the same trend within the statistical fluctuations. Using the values of $A_{0,2}$ parameters, considering the ^{5}He + α channel, we see in Fig. 9(d) that the angular distribution splits in two components for $E_{\alpha\alpha} < 0.4$ MeV. Effectively, the lowest part of the $E_{\alpha\alpha}$ spectrum is populated for $\theta_2 \approx 180^\circ$ which populates the two components at small and large θ_1. This is inconsistent with the experimental data. The $A_{0,2}$ parameters are successful in reproducing the 1D projection, but then result in a discrepancy with the 2D projections, especially $E_{\alpha\alpha}$ vs θ_1. We have carried out checks to ensure that the above assumption is robust against uncertainties in the angular correlation function, even though we have no reason to doubt the theoretical ones. It has been concluded that more isotropic angular correlation functions cannot satisfactorily reproduce the $E_{\alpha\alpha}$ distribution.

In order to estimate the possible ^{5}He + α strength we tried to deconvolute the two components in the θ_1 distribution with the condition 0.15 MeV $< E_{\alpha\alpha} <$ 0.35 MeV. But, as shown in Fig. 9, θ_1 measured in the experimental data has no energy dependence and the contribution of ^{5}He can only be buried in the statistical fluctuations. In this way, an upper limit of 2.5% can be estimated for the ^{5}He + α channel.

IV. DISCUSSION

The microscopic cluster model calculations of Descouvemont [10] provide partial widths for the two-body configurations for the low lying states of the mirror nuclei ^{9}Be and ^{9}B. In order to compare these to experiment, the given widths have to be folded with the decay penetrability appropriate to the given channel. This is presented in Table II where we compare the theoretical predictions with the experimentally observed strengths. In agreement with the experiment, the main strength is predicted to decay via the $^8\mathrm{Be}^{2^+} + n$ channel. However, the partial width of the ^{5}He + α channel is overestimated compared with the upper limit estimated to be $\Gamma < 2.5\%$ and probably much smaller. On the other hand, the $^8\mathrm{Be}^{0^+} + n$ partial width is underestimated with a factor of nearly 10. The ratio measured in previous work of $\approx 7\%$ indicates a stronger $^8\mathrm{Be}^{0^+} + n$ configuration of the 2.429 MeV state. This can be understood as this state is part of the rotational band based on the ground state expected, in the same reference, to have a dominant $^8\mathrm{Be}^{0^+} + n$ cluster configuration.

V. CONCLUSIONS

In this paper we have made measurements of the partial decay width for the 2.429 MeV state in ^{9}Be which is relevant for the astrophysically important three-body $\alpha + \alpha + n$ reaction.

The partial width of the $^8\mathrm{Be}^{0^+} + n$ channel has been measured and found consistent with previous work. The distinction between $^8\mathrm{Be}^{2^+} + n$ and $^5\mathrm{He}^{\mathrm{g.s.}} + \alpha$ channels has been made possible by an exclusive measurement, detecting and analyzing three particle events in a break-up reaction. The contribution of the "democratic" decay was not considered in this work.

The measurements show that the ^{5}He + α channel is not important for this state, although it is for higher states, see [26,27], but that the main decay is through the tail of the broad $J^\pi = 2^+$ state in ^{8}Be. A lack of counts in the present measurement precludes the same analysis being applied to the other two low-lying states, but with increased statistics it should be possible.

The present results indicate that the $^8\mathrm{Be}^{2^+} + n$ configuration is important in ^{9}Be and so should be included in any calculation of the $\alpha + \alpha + n$ reaction rate. The recent study by Prezado [18] showed it is also important for the next higher state at $E_x = 2.78$ MeV, which also has an appreciable ^{5}He + α configuration.

However, this poses a considerable theoretical challenge, since in both cases the intermediate states are broad and the usual narrow-resonance formalism cannot be applied. Some work in this direction has been reported recently [15,31] which suggests a small influence of the broad $^8\mathrm{Be}^{2^+}$ and $^5\mathrm{He}^{\mathrm{g.s.}}$ resonances. But, until rigorous calculations are available, it will not be possible to determine the extent to which these other configurations influence the astrophysical systems. This theoretical challenge needs to be addressed and, until it is, calculations of the $\alpha + \alpha + n$ reaction rate should be treated with caution.

ACKNOWLEDGMENTS

We would like to acknowledge P. Descouvemont for valuable discussions and help concerning penetrability calculations. This work was funded by the United Kingdom Engineering and Physical Sciences Research Council. The assistance of the staff at the Australian National University 14UD tandem facility is gratefully acknowledged.

[1] S. E. Woosley and R. D. Hoffman, Astrophys. J. **395**, 202 (1992).
[2] B. S. Meyer, G. J. Mathews, W. M. Howard, S. E. Woosley, and R. D. Hoffman, Astrophys. J. **399**, 656 (1992).
[3] W. M. Howard, S. Goriely, M. Rayet, and M. Arnould, Astrophys. J. **417**, 713 (1993).
[4] S. E. Woosley, J. R. Wilson, G. J. Mathews, R. D. Hoffman, and B. S. Meyer, Astrophys. J. **433**, 229 (1994).
[5] S. Dixit *et al.*, Phys. Rev. C **43**, 1758 (1991).
[6] C. Angulo *et al.*, Nucl. Phys. **A656**, 3 (1999).

[7] G. B. Caughlan and W. A. Fowler, At. Data Nucl. Data Tables **40**, 283 (1988).
[8] V. D. Efros, H. Oberhummer, A. Pushkin, and I. J. Thompson, Eur. Phys. J. A **1**, 447 (1998).
[9] J. Gorres, H. Herndl, I. J. Thompson, and M. Wiescher, Phys. Rev. C **52**, 2231 (1995).
[10] P. Descouvemont, Eur. Phys. J. A **12**, 413 (2001).
[11] K. Arai, P. Descouvemont, D. Baye, and W. N. Catford, Phys. Rev. C **68**, 014310 (2003).
[12] E. Gete *et al*., Phys. Rev. C **61**, 064310 (2000).
[13] L. Buchmann, E. Gete, J. C. Chow, J. D. King, and D. F. Measday, Phys. Rev. C **63**, 034303 (2001).
[14] K. Sumiyoshi, Nucl. Phys. **A709**, 467 (2002).
[15] L. V. Grigorenko and M. V. Zhukov, Phys. Rev. C **72**, 015803 (2005).
[16] O. Yu. Vasilev, A. A. Korsheninnikov, I. G. Mukha, and L. V. Chulkov, Pis'ma Zh. Eksp. Teor. Fiz. **49**, 539 (1989) [JETP Lett. **49**, 622 (1989)].
[17] O. V. Bochkarev *et al*., Sov. J. Nucl. Phys. **52**, 964 (1990) [Yad. Fiz. **52**. 1525 (1990)].
[18] Y. Prezado *et al*., Phys. Lett. **B618**, 43 (2005).
[19] B. R. Fulton *et al*., Phys. Rev. C **70**, 047602 (2004).
[20] H. Utsunomiya *et al*., Phys. Rev. C **63**, 018801 (2001).
[21] P. R. Christensen and C. L. Cocke, Nucl. Phys. **89**, 656 (1966).
[22] C. L. Cocke and P. R. Christensen, Nucl. Phys. **A111**, 623 (1968).
[23] G. Nyman *et al*., Nucl. Phys. **A510**, 189 (1990).
[24] J. Mösner, G. Schmidt, and J. Schintlmeister, Nucl. Phys. **64**, 169 (1965).
[25] N. Ashwood *et al*., Phys. Rev. C **72**, 024314 (2005).
[26] Y. Prezado *et al*., Phys. Lett. **B576**, 55 (2003).
[27] T. A. D. Brown *et al*., Break-up path measurements for states in ^{9}Be up to 11 MeV, submitted to Phys. Rev. C (2006).
[28] P. Papka, SIMSORT (unpublished).
[29] L. C. Biedenharn and M. E. Rose, Rev. Mod. Phys. **25**, 729 (1953).
[30] M. J. G. Borge *et al*., Phys. Scr. T **125**, 103 (2006).
[31] L. V. Grigorenko, Yu. L. Parfenova, and M. V. Zhukov, Phys. Rev. C **71**, 051604(R) (2005).